Free Volume in Poly(ether imide) Membranes Measured by Positron Annihilation Lifetime Spectroscopy and Doppler Broadening of Annihilation Radiation

Madzarevic, Zeljka P.; Schut, Henk; Čížek, Jakub; Dingemans, Theo J.

DOI
10.1021/acs.macromol.8b01723

Publication date
2018

Document Version
Final published version

Published in
Macromolecules

Macromolecules

Cite This: Macromolecules 2018, 51, 9925−9932

Article

pubs.acs.org/Macromolecules

Free Volume in Poly(ether imide) Membranes Measured by Positron Annihilation Lifetime Spectroscopy and Doppler Broadening of Annihilation Radiation

Zeljka P. Madzarevic,[†,‡] Henk Schut,[§] Jakub Čížek,[∥] and Theo J. Dingemans*[,†,⊥]

[†]Faculty of Aerospace Engineering, Novel Aerospace Materials, Delft University of Technology, Kluyverweg 1, 2629HS Delft, The Netherlands

[‡]Dutch Polymer Institute (DPI), P.O. Box 902, 5600AX Eindhoven, The Netherlands

[§]Faculty of Applied Sciences, Delft University of Technology, Mekelweg 15, 2629, JB Delft, The Netherlands

[∥]Faculty of Mathematics and Physics, Charles University, V Holešovičkách 2, CZ-18000 Praha 8, Czech Republic

[⊥]Department of Applied Physical Sciences, University of North Carolina at Chapel Hill, 1113 Murray Hall, 121 South Road, Chapel Hill, North Carolina 27599-3050, United States

ABSTRACT: In order to characterize the free volume of a homologous series all-aromatic poly(ether imide) (PEI) membranes, two positron annihilation techniques were utilized: positron annihilation lifetime spectroscopy (PALS) and Doppler broadening (DB) of annihilation radiation. First, DB, which is a fast and convenient method, indicated differences in free volume of all PEIs investigated, whereas PALS experiments gave more quantitative information, with respect to the size and distribution of the voids. DB results show that *S*, *W* pairs for this PEI-series tend to group according to their dianhydride moiety, meaning that, in this series, dianhydrides govern the differences in the *S* parameter, indicating more free volume with increasing *S* value. The semicrystalline PEI samples exhibit the lowest *S* parameter, while the amorphous samples based on 3,3′,4,4′-oxydiphthalic dianhydride (ODPA) all lie on the higher *S* side of the *S*−*W* plot. With the 1,4-bis(4-aminophenoxy)benzene (P1)-based PEI (ODPA-P1) standing out with the highest *S* parameter. The same could be confirmed and quantified by PALS, where ODPA-P1 is the only membrane in this series with its free volume described by both smaller and larger free-volume elements. The larger voids in ODPA-P1 can be characterized as having a radius (*R*) of 3.3 Å, which is 5 times larger than the lowest measured free-volume content in this series observed for 3,3′,4,4′-biphenyltetracarboxylic dianhydride (BPDA) and 1,3-bis(4-aminophenoxy)benzene (M1)-based PEI (BPDA-M1), which has voids with a radius of $R \approx 0.7$ Å. When comparing results obtained by DB and PALS, a very good correlation is observed between the *S* parameter (determined by DB) and the free-volume content (quantified by PALS).

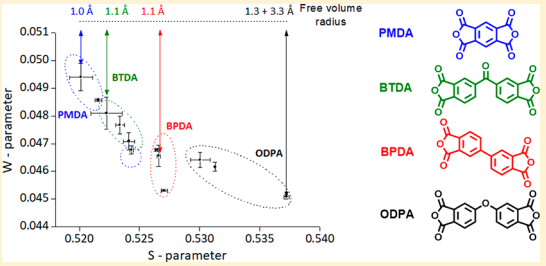

INTRODUCTION

Glassy polymers are nonequilibrium systems where excess free volume exists.[1] This excess free volume is kinetically confined within the polymer matrix, because of a rapid increase in the polymer chain relaxation upon vitrification. Essentially, because of the excess free volume, the polymer effectively becomes a two-component system: an equilibrium polymer matrix containing an additional void fraction.[2]

While the relaxation behavior of polymers is well-understood,[3] only limited information is available about the free volume. What are the dimensions of the voids? What is their distribution, in terms of size and shape?[4] This is primarily due to a lack of suitable techniques to probe open volumes of such dimensions. In this work, we report the free volume of a homologous series of prototypical poly(ether imide) (PEI) membranes, as measured using two different positron annihilation techniques: positron annihilation lifetime spectroscopy (PALS) and Doppler broadening (DB) of annihilation radiation. Both techniques enable monitoring of the free volume in polymers, in a nondestructive way and at the atomic level.[5−12] Free-volume data obtained by PALS have been effectively linked with transport properties of polymer membranes.[10−17]

In particular, PALS has developed into a very powerful technique for studying the free volume in polymers.[5−8] In work by Dlubek et al., polyimides and poly(etherimide)s were studied using a variable-energy positron beam, in combination with a DB technique.[18] The polymers were irradiated with B ions, which changes the polymer structure and composition. With this method, they could profile the modification depth or damage depth, since the penetration depth of positrons can be controlled. Inhibition of positronium formation by polar groups in Kapton and PMMA was studied by Shantarovich et al.,[19] using coincidence Doppler broadening (CDB).

Received: August 9, 2018
Revised: November 5, 2018
Published: November 29, 2018

DOI: 10.1021/acs.macromol.8b01723
Macromolecules 2018, 51, 9925−9932

Polyimide Kapton has a higher permeability for oxygen and a higher free volume. On the CDB ratio curve, Kapton shows a high momentum component typical for positron annihilation on oxygen. Recently, Chung and Le[20] characterized the mean depth profiles of dual-layer hollow fibers by $2\gamma/3\gamma$ annihilation ratio measurements. This polymer blend of polyimide and sulfonated polyimide has been investigated as a layer for ethanol dehydration, and this method was used to validate the change in the structure of the water-selective layer. A paper by Eastmond et al.[7] reported that there is a correlation between the void structure measured by PALS and the gas permeability of poly(etherimide)s. Positron lifetimes and intensities differ systematically with variations in polymer backbone structure and composition and, therefore, is ideal to study the relationship between permeability and separation of CO_2 and CH_4 in polymer-based membranes. The experimentally measured lifetimes represent the average of (assumed) spherical free-volume elements, where the larger lifetime values correspond to a larger free-volume elements.[10] Although a good deal of PALS experiments have been reported on PEIs, thus far, a methodical study on a systematic series of all-aromatic PEI-based membranes is lacking. Furthermore, a detailed study on how DB can be used to study the free volume in polymers is missing. In this work, we report the results of a comparative DB and PALS study.

THEORY BEHIND POSITRON ANNIHILATION TECHNIQUES

The antimatter counterpart of an electron, a *positron*, is generated by positron emission radioactive decay from a radioactive source, usually ^{22}Na. In polymers, a positron may form a system called *positronium* (Ps), which is a hydrogen-like bound state comprised of an electron and a positron. Ps is formed in two states in a 3:1 ratio, consisting of *ortho*-positronium (o-Ps, a parallel spin complex of a positron and an electron) and *para*-positronium (p-Ps, an antiparallel spin complex), shown in Figure 1. The intrinsic lifetimes of o-Ps and p-Ps (i.e., vacuum lifetimes) are 142 ns and 125 ps, respectively.

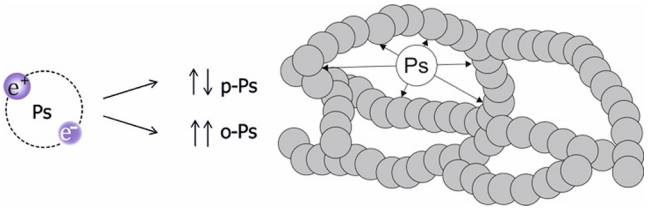

Figure 1. Positronium formation and localization in a void of the polymer's free volume. When an electron and a positron have parallel spin states, they can combine to form *ortho*-positronium (o-Ps), which can have a lifetime on the order of nanoseconds in electron-deficient regions of a polymer (i.e., free-volume elements).[4,21]

Para-Ps decays into two 511 keV annihilation photons, while o-Ps intrinsically decays into three annihilation photons with energies distributed from 0 to 511 keV. However, during the many collisions that o-Ps undergoes with the surrounding polymer, it has a finite probability of annihilation with an opposite spin electron from the surrounding polymer, which is a process known as the *pick-off*.[4]

Because of the change in electron spin, two 511 keV photons are emitted. A third o-Ps annihilation mode is via conversion to p-Ps through an exchange of the parallel spin electron of o-Ps with an antiparallel spin electron from the surrounding polymer. This p-Ps then self-decays within 125 ps via two-photon emission. Both the pick-off and exchange reaction compete with the o-Ps self-annihilation and sharply reduces the long o-Ps lifetime to typically 1−3 ns, depending on the collision frequency.[18,21] Positrons that do not form a positronium are annihilated with an electron of the atoms of the polymer molecules.

In polymers, the lifetime component associated with this direct two-photon annihilation mode lies between 200 ps and 400 ps. The collision frequency of the Ps with the surrounding polymer atoms will be dependent on the dimensions of the confining volume. This results in a highly sensitive correspondence of the o-Ps pick-off and exchange rate (and thus the lifetime) to the free-volume void size.[22,23−25] In a so-called "delayed coincidence" PALS experiment (Figure 2), we

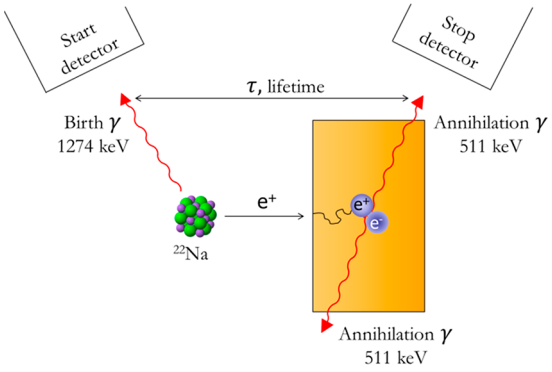

Figure 2. Schematic overview of a PALS experiment. The time between detecting a pair of signals from the emission of a positron, emanating from a radioactive source (^{22}Na), and the detection of annihilation gammas corresponds to the *lifetime* of a positron or a positronium (τ).

measure pairs of "start" and "stop" signals. For each pair, the time interval between the detection of the 1.27 MeV photon, emitted by ^{22}Na almost simultaneously with the positron, and the 511 keV annihilation photon is determined. By accumulating many of the delayed coincidence events (typically $>10^6$), a lifetime spectrum is obtained, which consists of several exponentially decaying lifetime components with corresponding intensities.[22,23]

As a result of momentum conservation during the above-mentioned two-photon annihilation processes (i.e., positrons that do not self-decay as o-Ps), the measured energy of annihilation photons is shifted by an amount ΔE, given by

$$\Delta E = \pm p\left(\frac{c}{2}\right) \quad (1)$$

where c is the speed of light and p the momentum component of the *electron* in the direction of photon emission. In an annihilation photon energy spectrum, these shifts give rise to a *Doppler broadening* of the 511 keV photo peak. Compared to annihilation of positrons from the free (nontrapped) state, trapping of positrons in open-volume defects increases the fraction of low-momentum valence electrons taking part in the direct annihilation process at the cost of reducing the fraction of annihilations with the higher momentum core electrons. In addition, in polymers, the decay of p-Ps exhibits an even narrower energy distribution, because of its intrinsic low

DOI: 10.1021/acs.macromol.8b01723
Macromolecules 2018, 51, 9925−9932

electron-positron momentum. Since Ps is formed more readily in regions with low electron density, such a narrow distribution can suggest the presence of an open volume.[26−28]

The Doppler broadening of the 511 keV photo peak is quantified by two specific line-shape parameters: the shape parameter (S) and the wing parameter (W) (shown in Figure 3). The shape parameter S gives the area under the curve

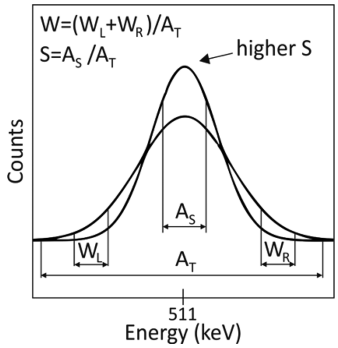

Figure 3. Doppler broadening of the 511 keV photo peak. The S parameter is defined as the ratio of the central peak area (A_S) to the total area (A_T), while the W parameter is defined as the ratio of the tail areas (W_L + W_R) to the total peak area.[28]

immediately around the peak (A_S) and the wing parameter W gives the area under the left and right wings of the curve (W_L + W_R), both normalized to the total area (A_T). The S parameter involves annihilations with low momentum electrons, while the W parameter is sensitive to annihilations with the high momentum outer shell core electrons. In regions with lower electron density, causing localization or trapping of positrons, the probability of annihilation with low momentum electrons is higher and therefore the S parameter increases. In addition, as the free volume size increases, the probability of outer shell core electron annihilation decreases. Because of these two effects and the possibility of formation and annihilation of p-Ps, a larger S parameter relates to a larger number and/or size of the free-volume voids. Given the definitions of S and W, an increase is S is accompanied by a decrease in W and the ratio R, which is defined as

$$R = \left|\frac{S - S_b}{W - W_b}\right| = \left|\frac{S_d - S_b}{W_d - W_b}\right| \quad (2)$$

can be defined with S_b and S_d, which represent the parameters for positrons annihilating from the free state, and W_b and W_d, which are the parameters for positrons annihilating from the trapped state, respectively. Since the atomic number of the atom involved dictates the momentum distribution density of these bound electrons, an additionally observed change in W (and, thus, R) may indicate a different chemical surrounding experienced by the positron or a different annihilation process, i.e., via the formation of Ps.[29]

EXPERIMENTAL SECTION

Doppler Broadening (DB) Spectroscopy. In this study, the DB experiments were performed with the Delft Variable Energy Positron (VEP) beam. All membranes were cut into single square sheets with dimensions of 20 mm × 20 mm × 0.03 mm and were easily mounted on a sample holder, which was then placed in the target chamber. Five different samples can be mounted each time and measured at one time. Positrons emitted from a radioactive ^{22}Na source are, after moderation to thermal energies and subsequent acceleration, injected in the PEI films with a kinetic energy ranging from 100 eV to 25 keV. The beam intensity is ∼10^4 positrons per second, and the beam diameter at the target is ∼8 mm. The mean implantation depth of the positrons ⟨z⟩ scales with the implantation energy, according to[30]

$$\langle z \rangle = \left(\frac{A}{\rho}\right) E^{1.62} \quad (3)$$

Here, A is a material-independent parameter ($A = 4.0 \times 10^{-6}$ g cm^{-2} keV$^{-1.62}$), ρ the density of the polymer (g/cm^3), and E the positron implantation energy (keV). In the polymers with a density of ∼1.4 g/cm^3, the mean implantation depth for 25 keV positrons is ∼5 μm. As the thinnest sample had a thickness of 7 μm, the DB data were taken at a mean implantation depth of ∼2 μm (the energy of implanted positrons is 14 keV) to avoid contributions of positrons implanted in the vicinity of the front- or backside surface. Sample preparation is simple, as only one thin film will suffice.

The S parameter was calculated as the ratio of the counts registered in a fixed central momentum window ($|p| < 3.5 \times 10^{-3}\ m_o c$) to the total number of counts in the annihilation photo peak. This choice of the momentum window makes the S parameter sensitive to annihilations with low-momentum valence electrons or p-Ps self-annihilation. Similarly, the W parameter is obtained from the high momentum regions (W_{left} and W_{right}) ($10 \times 10^{-3}\ m_o c < |p| < 26 \times 10^{-3}\ m_o c$) and accounts for annihilations with high-momentum outer-shell core electrons. The energy resolution of the detector setup is 1.2 at 511 keV. DB measurements were performed at 25 °C.

Positron Annihilation Lifetime Spectroscopy (PALS). Positron lifetime measurements were performed with the digital positron lifetime spectrometer at Charles University, as described in detail elsewhere,[31] with a time resolution of 143 ps full width at half-maximum (fwhm) of the resolution function. The resolution function was obtained by fitting the positron lifetime spectrum of a well-annealed Mg reference sample, which exhibits a single-component PALS spectrum (except of the source contribution) with a lifetime of 225 ± 1 ps. At least 10^7 annihilation events were accumulated in each positron lifetime spectrum. PALS measurements were performed in duplo at 25 °C.

Sample preparation can be described as follows. A $^{22}Na_2CO_3$ positron source (2 mm in diameter) with an activity of ∼1 MBq was deposited on a 2-μm-thick Mylar foil, sandwiched between two stacks of 20 mm × 20 mm polymer films (held together by a Kapton casing), each ∼0.6 mm thick, ensuring that a minimum of 93% of positrons from the source annihilate within the sample (Figure 4).

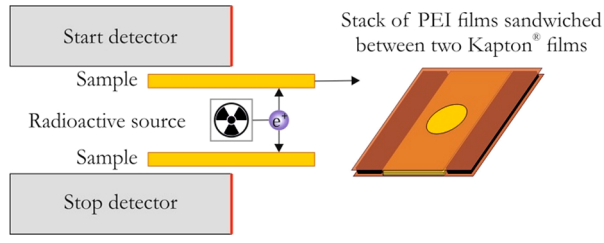

Figure 4. PALS was performed by sandwiching a radioactive source with stacks of polymer film samples from both sides and counting the positron formation (start) and annihilation (stop) events that occur within the analyte.

Since our 12 PEI films have different thicknesses (varying from 10 μm to 35 μm), the number of films in the stacks varied between 18 and 50 to ensure a minimum thickness of 0.6 mm. The source contribution was determined from fitting the PALS spectrum of the reference Mg sample. Intensity of the source contribution was recalculated for the Z number of studied samples, according to the formula described elsewhere.[32] The source contribution consists of two components: the positron annihilation within the $^{22}Na_2CO_3$ source itself and o-Ps pick-off annihilation in the Mylar film, with lifetimes of 368 ps and 1 ns, respectively, and relative intensities of

DOI: 10.1021/acs.macromol.8b01723
Macromolecules 2018, 51, 9925−9932

7.2% and 0.3%, respectively. Collected PALS spectra were deconvoluted to three exponential components, using a dedicated maximum likelihood code.[33] Each component is characterized by its lifetime and relative intensity. From the o-Ps lifetime data, an estimate of the characteristic radius of a free-volume element in the polymer is obtained by using the Tao−Eldrup model. In this model, the repulsive interaction of a Ps atom with the surrounding medium (the polymer) is approximated by a three-dimensional (3D) symmetrically infinite deep potential well (representing the free volume void) of radius R. The relationship between the observed reduced o-Ps lifetime and radius is then given by

$$\tau_{\text{o-Ps}} = \frac{1}{\lambda_A}\left[1 - \frac{R}{R+\Delta R} + \frac{1}{2\pi}\sin\left(2\pi\frac{R}{R+\Delta R}\right)\right]^{-1} \quad (4)$$

Here, $\tau_{\text{o-Ps}}$ is the reduced o-Ps lifetime and ΔR is the empirical electron layer thickness (ΔR = 1.66 Å).[34,35]

The parameter λ_A is the spin-averaged Ps annihilation rate under vacuum ($\lambda_A = \frac{\lambda_{p-Ps} + 3\lambda_{o-Ps}}{4} = 2\ \text{ns}^{-1}$), with $\lambda_{\text{p-Ps}}$ being the annihilation rate of the singlet state and $\lambda_{\text{o-Ps}}$ the annihilation rate of the triplet state. In the case of the ODPA-P1 sample, it was necessary to use two positronium components in order to achieve a good fit.

The average volume of the free-volume elements (V_{FVE}), can be calculated using eq 5.[36]

$$V_{\text{FVE}} = \left(\frac{4\pi}{3}\right)R^3 \quad (5)$$

The fractional free volume (FFV) is then proportional to the product of V_{FVE} and $I_{\text{o-Ps}}$:

$$\text{FFV} = kV_{\text{FVE}}I_{\text{o-Ps}} \quad (6)$$

where k is a scaling parameter whose value has been experimentally determined to be 0.018 nm^{-3}.[11,21,37] Nevertheless, the chemical nature of the polymer, evidently those containing electron-withdrawing groups, can inhibit the formation of o-Ps, therefore $I_{\text{o-Ps}}$ would not be indicative of the concentration of free-volume elements in the polymer.[12,15,21,38] In polyimides, the formation of Ps is strongly inhibited by the presence of O atoms in the conjugated five-membered imide moiety, since oxygen is known to be a strong positron scavenger, reducing the chance of Ps formation.[16] A well-known example is Kapton, in which Ps is not observed.

Materials. For this study, we used a homologous series of 12 prototypical poly(ether imide) (PEI) membrane films, as shown in Scheme 1. The synthesis details, thermomechanical properties, and membrane performance are described elsewhere.[39] Structures of the diamines were designed so that they have a *para*-, *meta*-, or *ortho*-based aryl ether "flexible" spacer unit between the two terminal *p*-phenylamine functionalities (Scheme 1).

The selected diamines are 1,4-bis(4-aminophenoxy)benzene (denoted as P1), 1,3-bis(4-aminophenoxy)benzene (denoted as M1), and 1,2-bis(4-aminophenoxy)benzene (denoted as O1). Changing the exocyclic bond angle in this three-ring diamine changes the backbone from a more linear conformation to a more bend or kinked conformation. In addition, the (local) electrostatic dipole moment changes as the O atoms move closer to each other when moving from a *para*-substitution pattern to an *ortho*-substitution pattern.

Four different dianhydride moieties have been selected to systematically change the flexibility of the PEI backbone, to tailor the segmental mobility and the nonequilibrium excess free volume of the polymer (Scheme 1). Selected dianhydrides are pyromellitic dianhydride (PMDA), 3,3′,4,4′-biphenyltetracarboxylic dianhydride (BPDA), 3,3′,4,4′-benzophenonetetracarboxylic dianhydride (BTDA), and 3,3′,4,4′-oxydiphthalic dianhydride (ODPA). All ODPA-based PEI membranes are amorphous, while all PMDA-based ones are semicrystalline.

Gas separation measurements are described in detail elsewhere.[39] The membrane properties, CO_2 permeability (P_{CO_2}) and selectivity (α_{CO_2/CH_4}) measured at 10 bar of mixed feed can be found in Table 1, alongside the degrees of crystallinity.

Scheme 1. Chemical Structures of the PEI Series Used for Our Study

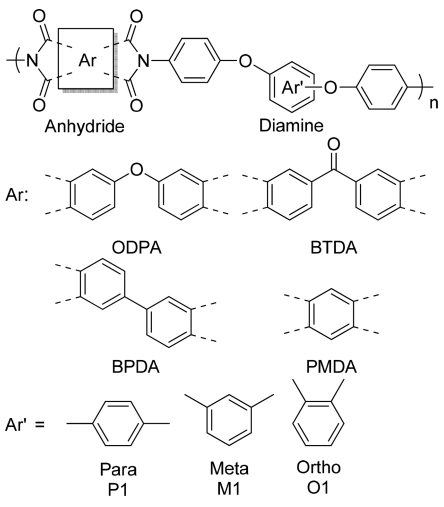

Table 1. Gas Transport Properties and Morphology of the PEI Membranes Used for This Study[a]

membrane	CO_2 permeability,[b] P_{CO_2} (Barrer)	selectivity,[b] α_{CO_2/CH_4} (−)	degree of crystallinity, ϕ_c (%)
ODPA-P1	0.62	48	0
BPDA-P1	0.27	44	6
BTDA-P1	0.49	43	18
PMDA-P1	1.63	36	19
ODPA-M1	0.29	68	0
BPDA-M1	0.09	58	3
BTDA-M1	0.09	59	6
PMDA-M1	–	–	11
ODPA-O1	0.50	53	0
BPDA-O1	1.07	72	0
BTDA-O1	0.32	73	0
PMDA-O1	–	–	4

[a]Data taken from ref 39. [b]Measured at 10 bar of CO_2/CH_4 (50/50) mixed feed at 35 °C.

RESULTS AND DISCUSSION

DB Spectroscopy. DB measurements on our 12 PEI films were performed in duplo at the Delft Variable Energy Positron beam facility. After analysis, data are presented in an $S-W$ map, as shown in Figure 5. It is immediately clear from this plot that the (S, W) pairs for these polymer are grouped according to their chemical composition. Looking at the S parameter, it seems that the major differentiator is the dianhydride moiety. The rigid PMDA-based PEI samples are located at the lower S and higher W side of the plot, while the flexible ODPA-based samples all lie on the higher S, lower W side; whereas the other two polymer groups (BPDA- and BTDA-based) are located between these entities. The resulting S parameter values, from low to high, follow the sequence PMDA ≈ BTDA > BPDA > ODPA. Recall that a high S value is associated with a narrow momentum distribution (i.e., enhanced contribution of positrons annihilated by low

DOI: 10.1021/acs.macromol.8b01723
Macromolecules 2018, 51, 9925−9932

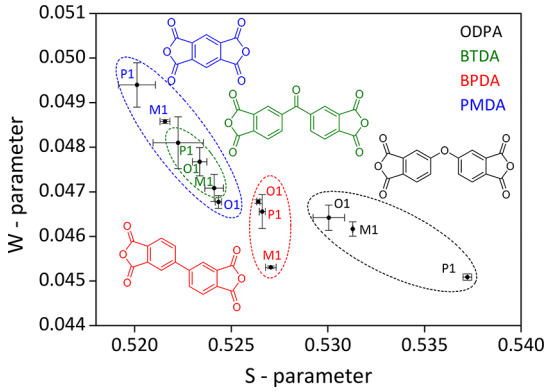

Figure 5. *S*–*W* plot from DB measurements showing the DB parameters of all 12 PEI film samples summarized in a single *S*–*W* map. Measurements were performed in duplo.

momentum electrons either via direct annihilation with valence electrons or through p-Ps decay). Hence, the sequence PMDA ≈ BTDA > BPDA > ODPA can be interpreted as reflecting an increase in free volume, either by size or by concentration.

Results of the gas separation measurements using the CO_2/CH_4 mixed feed, which have been discussed in detail elsewhere,[39] have shown that ODPA-P1 is the most-permeable membrane for CO_2 and the most-resistant one to CO_2 plasticization. The high permeability of this membrane is second to only the PMDA-P1 membrane. However, we found that the high permeability exhibited by PMDA-P1 stems from the sorption capacity of this membrane, not the free volume content measured for the virgin membrane. The high affinity of CO_2 toward the PMDA-P1 backbone[40] results in an increase of free volume by CO_2 sorption, leading to plasticization and an increase in gas permeation.[39] This correlates well with the DB results, where we identified PMDA-P1 as the material with the lowest amount of free volume, i.e., very similar to Kapton,[19] as was expected based on the backbone composition and chain packing ability. PMDA-P1 seems to be an outlier in the PMDA-based series, which is most likely the result of its all-rigid (linear) backbone configuration. In contrast, the M1 and O1 modifications are much more kinked (nonlinear).

On the other end of the spectrum, within the ODPA-based membrane series, ODPA-P1 stands out with the highest *S* value, compared to ODPA-M1 and ODPA-O1. This indicates that, in this group, the kinked diamines, and the associated larger local dipole moments, do not have much of an effect on the free volume. The most rigid and symmetric analogue within this group, ODPA-P1, does not crystallize and generates the most free volume. Generally, a prominent and rigid kink in the polymer backbone is expected to create more free volume in the material by inhibiting efficient chain packing;[8,41−43] however, M1 and O1 are not as rigid as P1, whose linear backbone, in combination with a flexible ODPA moiety, causes packing in such a way that it creates more free volume. The P1 diamine generates the most free volume, because rotation around the diamine Ar−O−Ar bonds does not change the overall shape of the moiety between the dianhydride oxygen bridges. In principle, an amorphous network is built using rigid rods of 25 Å (Scheme 2). The average length of the rods for M1 and O1 are shorter.

Positron Annihilation Lifetime Spectroscopy. In order to quantify the free-volume differences as observed by DB and to gain more insight into the free-volume size and distribution,

Scheme 2. Schematic Representation of the Structural Rigidity of the ODPA-P1 Repeating Unit and Rodlike Depiction of the P1 Moiety

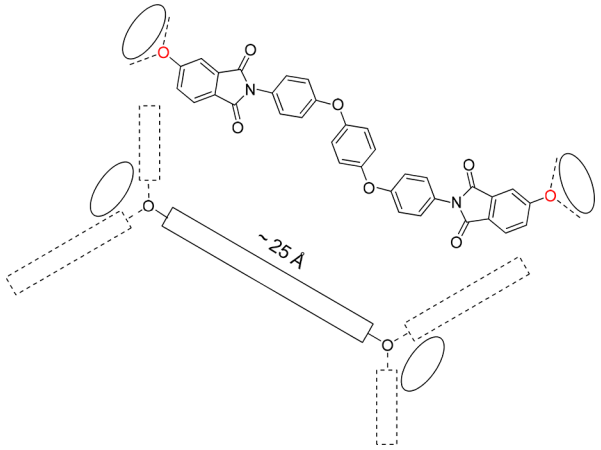

positron lifetime experiments on selected samples have been conducted. Table 2 shows the PALS results for 10 PEI films. Polymer films of PMDA-M1 and PMDA-O1 are very brittle and difficult to handle; therefore, it was not possible to stack enough defect-free films required for PALS experiments (unlike for DB, where only one defect-free film is sufficient). The shorter component with lifetime τ_1 and intensity I_1 represents a contribution from positrons annihilated as free particles, while the long-lived components $\tau_{o\text{-}Ps}$ are associated with the pick-up annihilation of ortho-Ps. The lifetime of p-Ps self-annihilation was fixed at 125 ps and the ratio of o-Ps to p-Ps contribution was kept at 3:1. In the table, I_{Ps} denotes the total intensity of the Ps contribution (i.e., p-Ps plus o-Ps). The mean size (radius *R*) of free volumes can be estimated using the Tao−Eldrup equation (eq 4) and is also given in Table 2. A first look at the P1-based series shows that, in the case of the ODPA-P1 membrane, it was necessary to use two Ps components in order to achieve a good fit. Hence, the ODPA-P1 sample exhibits two distinguishable free-volume elements:

(1) smaller ones, which are characterized by a o-Ps lifetime of $\tau_{o\text{-}Ps\text{-}1} \approx 0.80$ ns, and
(2) larger ones, which are characterized by a o-Ps lifetime of $\tau_{o\text{-}Ps\text{-}2} \approx 2.3$ ns.

The other nine PEIs contain only the smaller open volumes, since the o-Ps component with a lifetime of 2.3 ns could not be detected. Moreover, the mean size of the smaller volumes in ODPA-P1 is larger than in the other three P1-based samples. In particular, the PMDA-P1 sample exhibits the smallest free-volume size among all P1-based samples studied ($\tau_{o\text{-}Ps\text{-}1} \approx 0.66$ ns, corresponding to $R \approx 0.1$ nm). In M1- and O1-based PEI membranes, it was interesting to see that the BTDA-M1 and BTDA-O1 PEIs do not show any o-Ps formation: the intensities were below the detection limit, similar to what was observed for Kapton,[19] which could suggest poor membrane performance. In the M1- and O1-based series, the ODPA-based PEI membranes have the highest free volume, which is actually higher than that of the "smaller volumes" of ODPA-P1. However, unlike ODPA-P1, these two do not exhibit the "larger type" free volumes. BPDA-O1 shows values in free-volume size similar to that of BPDA-P1 and BTDA-P1, while BPDA-M1 shows the lowest measurable free-volume

DOI: 10.1021/acs.macromol.8b01723
Macromolecules 2018, 51, 9925−9932

Table 2. Positron and o-Ps Lifetimes and Intensities, Average Radius of Free-Volume Elements, Average Volume of Free-Volume Elements, and Fractional Free Volume (FFV)[a]

membrane	τ_1 (ps)	I_1 (%)	$\tau_{o\text{-}Ps\text{-}1}$ (ns)	$I_{Ps\text{-}1}$ (%)	R_1 (nm)	V_{FVE} (nm^3)	FFV (%)	$\tau_{o\text{-}Ps\text{-}2}$ (ns)	$I_{Ps\text{-}2}$ (%)	R_2 (nm)	V_{FVE} (nm^3)	FFV (%)	goodness of fit,[b] χ^2/ν
ODPA-P1	363.3(3)	88.7(4)	0.80(3)	8.8(3)	0.13(1)	0.009(2)	0.15(3)	2.3(1)	2.5(1)	0.33(1)	0.151(1)	0.68(3)	1.02
BTDA-P1	361.4(2)	94.7(2)	0.715(9)	5.3(2)	0.109(8)	0.006(1)	0.05(1)	–	–	–	–	–	1.03
BPDA-P1	362.7(3)	95.5(3)	0.72(2)	4.5(3)	0.11(1)	0.006(2)	0.05(2)	–	–	–	–	–	1.02
PMDA-P1	371.5(3)	95.8(3)	0.66(2)	4.2(3)	0.10(1)	0.004(1)	0.03(1)	–	–	–	–	–	1.01
ODPA-M1	366.4(4)	96.0(1)	1.10(2)	4.0(2)	0.18(1)	0.025(4)	0.18(3)	–	–	–	–	–	1.03
BTDA-M1	369.8(3)	100	–	–	–	–	–	–	–	–	–	–	1.02
BPDA-M1	352.6(3)	89.9(6)	0.57(1)	10.1(3)	0.07(1)	0.001(1)	0.03(3)	–	–	–	–	–	1.01
ODPA-O1	368.6(4)	96.1(2)	1.15(2)	3.9(5)	0.19(5)	0.029(5)	0.20(4)	–	–	–	–	–	1.03
BTDA-O1	374.4(2)	100	–	–	–	–	–	–	–	–	–	–	1.01
BPDA-O1	367.0(3)	95.5(6)	0.77(4)	4.5(3)	0.12(2)	0.007(4)	0.06(3)	–	–	–	–	–	1.02

[a]The uncertainties (one standard deviation in the unit of the last significant digit) are given in parentheses. [b]The goodness-of-fit is expressed as the χ^2 value per the number of degrees of freedom (ν).

content in the entire series, characterized by a o-Ps lifetime of $\tau_{o\text{-}Ps\text{-}1} \approx 0.57$ ns, corresponding to a radius $R \approx 0.07$ nm. This is ~5 times smaller than the radius of the larger free volume observed for ODPA-P1 characterized with a radius of 0.33 nm (or 3.3 Å).

Analogous to the DB measurements, we observed that the free-volume radius results for this PEI series can also be grouped according to dianhydride moiety. With ODPA-based membranes exhibiting the highest free-volume radius, followed by significantly lower values for BPDA-based membranes and next to none for PMDA- and BTDA-based ones. The relationship between the DB and PALS measurements is visualized in Figure 6 by indicating the values of radii of free-volume voids R in the DB S–W plot. For the sake of clarity, we focused on the P1-based series. It shows a good correlation between the S parameter obtained by DB and free-volume radius obtained by PALS. The larger free volume void is indicated both with the enhanced S-parameter and the calculated radius.

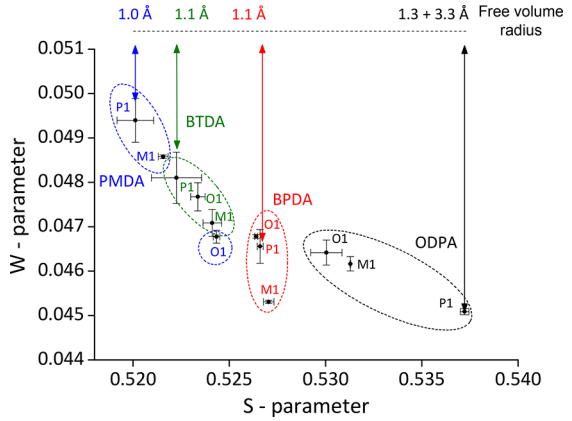

Figure 6. Free volume indicated by the DB S parameter and quantified by PALS, focusing on P1-based PEIs with four distinctive dianhydride moieties.

By plotting the o-Ps lifetime $\tau_{o\text{-}Ps\text{-}1}$ against the DB S parameter, a good agreement between the DB and PALS results was observed, as shown in Figure 7. The S parameter positively follows the trend of o-Ps lifetime, more so than the o-Ps intensity, and appears to be more affected by the amount of positronium formed.

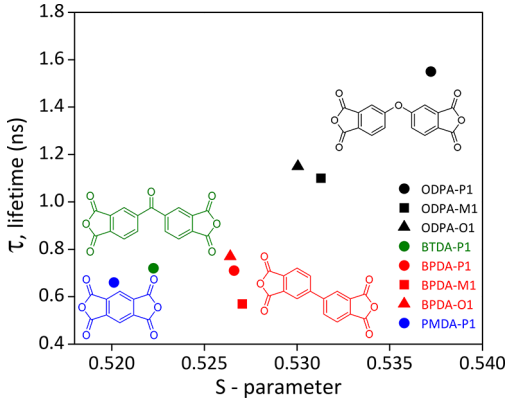

Figure 7. o-Ps lifetime $\tau_{o\text{-}Ps\text{-}1}$ vs S parameter.

DOI: 10.1021/acs.macromol.8b01723
Macromolecules 2018, 51, 9925–9932

Our poly(ether imide) PMDA-P1 has a structure very similar to that of Kapton, which is poly(4,4′-oxydiphenylene pyromellitimide) (PMDA-ODA), and, in our results, PMDA-P1 has the lowest *S* parameter value, confirming its similarity to Kapton. These two materials are both closely packed and semicrystalline and have poor membrane performances.

CONCLUSIONS

We have used PALS and DB to probe the free volume of a homologous prototypical series of all-aromatic poly(ether imide)-based membranes. Both techniques allowed us to probe the free volume of this important class of polymer membranes in a nondestructive manner and at the atomic level. Variable positron beam DB proved to be a fast and convenient method to assess the relative differences in free volume of the PEIs used for this study, with a minimal demand on sample preparation, where a single film is sufficient. The high-resolution ^{22}Na-source-based PALS experiments, on the other hand, gave more quantitative information, with respect to the size and number of Angstrom-scale voids. The downside of the setup used in this work is that it requires larger amounts of defect-free films that need to be stacked. From the DB experiments, the resulting *S*,*W* pairs for these polymers show a tendency to group according to their dianhydride composition, meaning that the dianhydride governs the differences in *S* parameter. The PMDA-based PEI samples are located at the lower *S* and higher *W* side of the plot, while the ODPA-based samples all lie on the higher *S*, lower *W* side with ODPA-P1 standing out, in terms of accessible free volume. The same trend was observed by PALS, where ODPA-P1 is the only polymer in the series with its free volume defined by both smaller and larger free-volume elements. These characteristics are quantified with an o-Ps lifetime component that can estimate the radius of the free volume in which the o-Ps resides, using the Tao−Eldrup model. In the case of ODPA-P1, the larger voids have a radius of 3.3 Å, which is 5 times larger than the lowest measured free-volume content in this series observed for BPDA-M1, which has a radius of $R \approx 0.7$ Å.

AUTHOR INFORMATION

Corresponding Author

*Tel.: +1(919) 843 4048. E-mail: tjd@unc.edu.

ORCID

Theo J. Dingemans: 0000-0002-8559-2783

Notes

The authors declare no competing financial interest.

ACKNOWLEDGMENTS

This research forms part of the research program of the Dutch Polymer Institute (DPI), Project No. 715. Financial support from the Czech Science Agency (Project No. 18-09347S) is gratefully acknowledged.

REFERENCES

(1) Tant, M. R.; Wilkes, G. L. An Overview of the Nonequilibrium Behavior of Polymer Glasses. *Polym. Eng. Sci.* **1981**, *21*, 874−895.

(2) Ogieglo, W.; Wormeester, H.; Wessling, M.; Benes, N. E. Effective Medium Approximations for Penetrant Sorption in Glassy Polymers Accounting for Excess Free Volume. *Polymer* **2014**, *55*, 1737−1744.

(3) Donth, E.; *The Glass Transition: Relaxation Dynamics in Liquids and Disordered Materials*; Springer−Verlag: Berlin, Germany, 2001; pp 149−157.

(4) Dlubek, G.; Kilburn, D.; Bondarenko, V.; Pionteck, J.; Alam, M. A. Characterisation of Free Volume in Amorphous Materials by PALS in Relation to Relaxation Phenomena. In *Proceedings of the 24th Arbeitskreistagung "Nichtkristalline Strukturen" of DGK*, Jena, Germany, Sept. 2003.

(5) Zhang, R.; Robles, J.; Kang, J.; Samha, H.; Chen, H. M.; Jean, Y. C. Study of the Chemical Environment inside Free Volume Holes in Halogenated Styrene Polymers Using Positron Annihilation Spectroscopy. *Macromolecules* **2012**, *45*, 2434−2441.

(6) Quarles, C. A.; Klaehn, J. R.; Peterson, E. S.; Urban-Klaehn, J. M.; McDaniel, F. D.; Doyle, B. L. Positron Annihilation Spectroscopy of High Performance Polymer Films Under CO_2 Pressure. *AIP Conf. Proc.* **2010**, *513*, 513−518.

(7) Eastmond, G. C.; Daly, J. H.; Mckinnon, A. S.; Pethrick, R. A. Poly(ether imide)s: Correlation of Positron Annihilation Lifetime Studies with Polymer Structure and Gas Permeability. *Polymer* **1999**, *40*, 3605−3610.

(8) Calle, M.; Doherty, C. M.; Hill, A. J.; Lee, Y. M. Cross-Linked Thermally Rearranged Poly(benzoxazole- Co -Imide) Membranes for Gas Separation. *Macromolecules* **2013**, *46* (20), 8179−8189.

(9) Rowe, B. W.; Pas, S. J.; Hill, A. J.; Suzuki, R.; Freeman, B. D.; Paul, D. R. A Variable Energy Positron Annihilation Lifetime Spectroscopy Study of Physical Aging in Thin Glassy Polymer Films. *Polymer* **2009**, *50*, 6149−6156.

(10) Hill, A. J.; Freeman, B. D.; Jaffe, M.; Merkel, T. C.; Pinnau, I. Tailoring Nanospace. *J. Mol. Struct.* **2005**, *739*, 173−178.

(11) Ju, H.; Sagle, A. C.; Freeman, B. D.; Mardel, J. I.; Hill, A. J. Characterization of Sodium Chloride and Water Transport in Crosslinked Poly(ethylene Oxide) Hydrogels. *J. Membr. Sci.* **2010**, *358*, 131−141.

(12) Xie, W.; Ju, H.; Geise, G. M.; Freeman, B. D.; Mardel, J. I.; Hill, A. J.; McGrath, J. E. Effect of Free Volume on Water and Salt Transport Properties in Directly Copolymerized Disulfonated Poly(arylene Ether Sulfone) Random Copolymers. *Macromolecules* **2011**, *44*, 4428−4438.

(13) Rowe, B. W.; Freeman, B. D.; Paul, D. R. Physical Aging of Ultrathin Glassy Polymer Films Tracked by Gas Permeability. *Polymer* **2009**, *50*, 5565−5575.

(14) Pethrick, R. A.; Santamaria-Mendia, F. Gas Permeation and Positron Annihilation Lifetime Spectroscopy of Poly(ether Imides) Containing Main Chain Ethylene Oxide Segments. *J. Polym. Sci., Part B: Polym. Phys.* **2015**, *53*, 1654−1662.

(15) Kobayashi, Y.; Mohamed, H. F. M.; Ohira, A. Positronium Formation in Aromatic Polymer Electrolytes for Fuel Cells. *J. Phys. Chem. B* **2009**, *113*, 5698−5701.

(16) Van Goethem, C.; Verbeke, R.; Pfanmöller, M.; Koschine, T.; Dickmann, M.; Timpel-Lindner, T.; Egger, W.; Bals, S.; Vankelecom, I. F. J. The Role of MOFs in Thin-Film Nanocomposite (TFN) Membranes. *J. Membr. Sci.* **2018**, *563*, 938−948.

(17) Koschine, T.; Rätzke, K.; Faupel, F.; Khan, M. M.; Emmler, T.; Filiz, V.; Abetz, V.; Ravelli, L.; Egger, W. Correlation of Gas Permeation and Free Volume in New and Used High Free Volume Thin Film Composite Membranes. *J. Polym. Sci., Part B: Polym. Phys.* **2015**, *53*, 213−217.

(18) Dlubek, G.; Börner, F.; Buchhold, R.; Sahre, K.; Krause-Rehberg, R.; Eichhorn, K.-J. Damage-Depth Profiling of Ion-Irradiated Polyimide Films with a Variable-Energy Positron Beam. *J. Polym. Sci., Part B: Polym. Phys.* **2000**, *38*, 3062−3069.

(19) Shantarovich, V. P.; Suzuki, T.; He, C.; Gustov, V. W. Inhibition of Positronium Formation by Polar Groups in Polymers—relation with TSL Experiments. *Radiat. Phys. Chem.* **2003**, *67*, 15−23.

(20) Le, N. L.; Chung, T.-S. High-Performance Sulfonated Polyimide/polyimide/polyhedral Oligosilsesquioxane Hybrid Membranes for Ethanol Dehydration Applications. *J. Membr. Sci.* **2014**, *454*, 62−73.

(21) Pethrick, R. A. Positron Annihilation - A Probe for Nanoscale Voids and Free Volume? *Prog. Polym. Sci.* **1997**, *22*, 1−47.

(22) For example, see: (a) *Positron and Positronium Chemistry*; Schrader, D. M., Jean, Y. C., Eds.; Elsevier: Amsterdam, 1988.

DOI: 10.1021/acs.macromol.8b01723
Macromolecules 2018, 51, 9925−9932

(b) *Principles and Applications of Positron and Positronium Chemistry*; Jean, Y. C., Mallon, P. E., Schrader, D. M., Eds.; World Scientific: Singapore, 2003.
(23) Mogensen, O. E. *Positron Annihilation Chemistry*; Springer−Verlag: Berlin, Germany, 1995; pp 15−28.
(24) Vleeshouwers, S.; Kluin, J.-E.; Mcgervey, J. D.; Jamieson, a. M.; Simha, R. Monte Carlo Calculations of Hole Size Distributions: Simulation of Positron Annihilation Spectroscopy. *J. Polym. Sci., Part B: Polym. Phys.* **1992**, *30*, 1429−1435.
(25) Schmitz, H.; Müller-Plathe, F. Calculation of the Lifetime of Positronium in Polymers via Molecular Dynamics Simulations. *J. Chem. Phys.* **2000**, *112*, 1040−1045.
(26) Kobayashi, Y. Positron Chemistry in Polymers. *Defect Diffus. Forum* **2012**, *331*, 253−274.
(27) Ruiz-Ripoll, M. L.; Schut, H.; Van Dijk, N. H.; Alderliesten, R. C.; Van Der Zwaag, S.; Benedictus, R. The Generation of Deformation Damage during Fatigue Loading in Al-Cu Alloy Studied by the Doppler Broadening Technique. *J. Phys. Conf. Ser.* **2011**, *262*, 012052.
(28) Choudalakis, G.; Gotsis, A. D.; Schut, H.; Picken, S. J. The Free Volume in Acrylic Resin/laponite Nanocomposite Coatings. *Eur. Polym. J.* **2011**, *47*, 264−272.
(29) Mantl, S.; Triftshäuser, W. Defect Annealing Studies on Metals by Positron Annihilation and Electrical Resitivity Measurements. *Phys. Rev. B: Condens. Matter Mater. Phys.* **1978**, *17*, 1645−1653.
(30) Mills, A. P.; Wilson, R. J. Transmission of 1−6-keV Positrons through Thin Metal Films. *Phys. Rev. A: At., Mol., Opt. Phys.* **1982**, *26*, 490−500.
(31) Bečvář, F.; Čížek, J.; Procházka, I.; Janotová, J. The Asset of Ultra-Fast Digitizers for Positron-Lifetime Spectroscopy. *Nucl. Instrum. Methods Phys. Res., Sect. A* **2005**, *539*, 372−385.
(32) von Surbeck, H. Lebensdauer der Positronen in Silberbromid. *Helv. Phys. Acta* **1977**, *50*, 705−721.
(33) Procházka, I.; Novotný, I.; Bečvár, F. Application of Maximum-Likelihood Method to Decomposition of Positron-Lifetime Spectra to Finite Number of Components. *Mater. Sci. Forum* **1997**, *255−257*, 772−774.
(34) Eldrup, M.; Lightbody, D.; Sherwood, J. N. The Temperature Dependence of Positron Lifetimesin Solid Pivalic Acid. *Chem. Phys.* **1981**, *63*, 51−58.
(35) Tao, S. J. Positronium Annihilation in Molecular Substances. *J. Chem. Phys.* **1972**, *56*, 5499.
(36) Yampolskii, Y.; Shantarovich, V. Positron Annihilation Lifetime Spectroscopy and Other Methods for Free Vol. Evaluation in Polymers. In *Materials Science of Membranes for Gas and Vapor Separation*; Yampolskii, Y., Pinnau, I., Freeman, B. D., Eds.; John Wiley & Sons: Chichester, U.K., 2006; pp 191−210.
(37) Jean, Y. C. Positron Annihilation Spectroscopy A Novel Probe for Microstructural for Chemical Analysis: Analysis of Polymers. *Microchem. J.* **1990**, *42*, 72−102.
(38) Hirata, K.; Kobayashi, Y.; Ujihira, Y. Effect of Halogenated Compounds on Positronium Formation in Polycarbonate and Polysulfone Matrices. *J. Chem. Soc., Faraday Trans.* **1997**, *93*, 139−142.
(39) Madzarevic, Z. P.; Shahid, S.; Nijmeijer, K.; Dingemans, T. J. The Role of Ortho-, Meta- and Para-Substitutions in the Main-Chain Structure of Poly(etherimide)s and the Effects on CO_2/CH_4 Gas Separation Performance. *Sep. Purif. Technol.* **2019**, *210*, 242−250.
(40) Ogieglo, W.; Madzarevic, Z. P.; Raaijmakers, M. J. T.; Dingemans, T. J.; Benes, N. E. High-Pressure Sorption of Carbon Dioxide and Methane in All-Aromatic Poly(Etherimide)-Based Membranes. *J. Polym. Sci., Part B: Polym. Phys.* **2016**, *54*, 986−993.
(41) Mercado, R.; Wang, Y.; Flaim, T.; Dimenna, W.; Senapati, U. Thin-Film Polyetherimides with Controlled Refractive Indices. *Proc. SPIE* **2004**, *5351*, 276−283.
(42) Ritter, N.; Senkovska, I.; Kaskel, S.; Weber, J. Intrinsically Microporous Poly (Imide) S: Structure− Porosity Relationship Studied by Gas Sorption and X-ray Scattering. *Macromolecules* **2011**, *44*, 2025−2033.
(43) Ghanem, B. S.; McKeown, N. B.; Budd, P. M.; Selbie, J. D.; Fritsch, D. High-Performance Membranes from Polyimides with Intrinsic Microporosity. *Adv. Mater.* **2008**, *20*, 2766−2771.

DOI: 10.1021/acs.macromol.8b01723
Macromolecules 2018, 51, 9925−9932